PHYSICAL REVIEW D **91,** 014005 (2015)

# Transverse single spin asymmetry in $e + p^{\uparrow} \to e + J/\psi + X$ and $Q^2$ evolution of Sivers function-II

Rohini M. Godbole,[1,*] Abhiram Kaushik,[1,†] Anuradha Misra,[2,‡] and Vaibhav S. Rawoot[2,§]

[1]*Centre for High Energy Physics, Indian Institute of Science, Bangalore 560012, India*
[2]*Department of Physics, University of Mumbai, Mumbai 400098, India*

(Received 12 June 2014; published 5 January 2015)

We present estimates of single spin asymmetry in the electroproduction of $J/\psi$ taking into account the transverse momentum-dependent (TMD) evolution of the gluon Sivers function. We estimate single spin asymmetry for JLab, HERMES, COMPASS and eRHIC energies using the color evaporation model of $J/\psi$. We have calculated the asymmetry using recent parameters extracted by Echevarria *et al.* using the Collins-Soper-Sterman approach to TMD evolution. These recent TMD evolution fits are based on the evolution kernel in which the perturbative part is resummed up to next-to-leading logarithmic accuracy. We have also estimated the asymmetry by using parameters which had been obtained by a fit by Anselmino *et al.*, using both an exact numerical and an approximate analytical solution of the TMD evolution equations. We find that the variation among the different estimates obtained using TMD evolution is much smaller than between these on one hand and the estimates obtained using DGLAP evolution on the other. Even though the use of TMD evolution causes an overall reduction in asymmetries compared to the ones obtained without it, they remain sizable. Overall, upon use of TMD evolution, predictions for asymmetries stabilize.

DOI: 10.1103/PhysRevD.91.014005 PACS numbers: 13.88.+e, 13.60.-r, 14.40.Lb, 29.25.Pj

## I. INTRODUCTION

There has been a lot of work done lately on the phenomenology of TMDs (transverse momentum-dependent parton distribution functions (PDFs), fragmentation functions, etc.), their measurement and $Q^2$ evolution [1,2]. TMDs give details of the intrinsic transverse momenta of partons, providing an understanding of the three-dimensional structure of nucleons. Their $Q^2$ evolution has nonperturbative contributions as opposed to the evolution of collinear distributions, which is completely perturbative. A knowledge of the TMDs can be obtained by using the single spin asymmetries (SSAs) observed in scattering experiments involving a single transversely polarized hadron [3–5]. These include Drell-Yan scattering and semi-inclusive deep inelastic scattering (SIDIS). One of the ways to analyse these SSAs is based on a transverse momentum-dependent factorization scheme. Such a scheme was first provided by Collins and Soper [6,7], which has, since then, been used to study the above processes. In TMD factorization, the transverse momenta of the partons are not integrated over, as they are in the standard collinear factorization schemes of QCD.

One of the most important SSAs is the Sivers asymmetry. It is due to a TMD called the Sivers function, which gives the probability of finding an unpolarized parton inside a transversely polarized nucleon. Many fits of the Sivers function are available which are extracted from experimental data of SIDIS from the HERMES, COMPASS and JLAB experiments [8,9]. The most recent fit, which we use in this paper, is by Echevarria *et al.* [10] who have fitted the Sivers function in the Torino parametrization, one of the two commonly used parametrizations of the Siver function, the other being the Bochum parametrization [2]. We have exclusively used the Torino parametrization in this as well as our previous works on the subject. Echevarria *et al.* have performed a global fit to all the experimental data on SIDIS from HERMES [11], COMPASS [12,13] and JLAB [14] experiments. They have used the Sivers function fits so obtained to make predictions for the Sivers asymmetry in Drell-Yan and $W^+$ and $W^-$ boson production. These predictions agree well with data, giving a $\chi^2/\text{d.o.f} \approx 1.3$. Previous fits given by Anselmino *et al.* [15] had extracted the Sivers function in SIDIS data from the HERMES [11] and COMPASS [16] experiments alone. The earliest fits of the Sivers function had assumed that the transverse momentum behavior factorized from the collinear distributions and did not evolve. This may be a reasonable approximation to make for low $Q^2$ processes but is not valid for high $Q^2$ processes as was the case for COMPASS data.

Both fits by Echevarria *et al.* and Anselmino *et al.*, used here, incorporate the evolution of the transverse momentum dependence. The Echavarria *et al.* fits differ from the Anselmino *et al.* fits in two aspects: First, they use a certain prescription for the initial scale of the evolution kernel explained in Ref. [10] in order to simplify the evolution equations, and second, their kernel is consistently resummed to next-to-leading-logarithmic (NLL) accuracy.

*rohini@cts.iisc.ernet.in
†abhiramb@cts.iisc.ernet.in
‡misra@physics.mu.ac.in
§vaibhavrawoot@gmail.com

 

In the present work, we make predictions for Sivers asymmetry in low virtuality electroproduction of $J/\psi$, using the latest fits by Echevarria *et al.* [10]. The present work deals with the gluon Sivers asymmetry in the leptoproduction of charmonium.

The leptoproduction of heavy flavors (open and closed) in general, and of charmonium, in particular, is a direct probe of the gluon content of the proton. At leading order, this involves a gluon and a photon fusing to form a $c\bar{c}$ pair. It was first studied in this context in Ref. [17]. In our earlier work, we had extended the idea to the case of the gluon Sivers function [18,19]. We had made predictions for Sivers asymmetry in the process $e + p^{\uparrow} \to e + J/\psi + X$, first using DGLAP evolved TMDs [18] and later PDFs and the Sivers function taking evolution of the transverse momentum distribution into account [19]. In this paper, we would like to assess the dependence of asymmetries on the different aspects of the implementation of the QCD evolution of TMDs. The estimates in Ref. [19] were based on a formalism given by Anselmino *et al.* where they had used an analytical solution of an approximate form of the TMD evolution equation [15]. In the current work, we use the exact treatment of TMD evolution. Second, we also use a new parametrization of the Sivers function obtained from fits performed with a NLL resummed evolution kernel [10]. We give revised estimates of the Sivers asymmetry in charmonium leptoproduction.

It must be mentioned here that there is no direct experimental information available on the gluon Sivers function. Boer and Vogelsang [20] proposed an ansatz for the gluon Sivers function, and it was parametrized in terms of quark Sivers function parameters which in turn are extracted by fitting the observed asymmetries in SIDIS. They also used this ansatz to make predictions for asymmetry in dijet production at relativistic heavy ion collider (RHIC). We have used their model to get our estimates in this and the earlier work on charmonium [18,19]. We thus estimate the size of the asymmetry under two plausible parametrizations of the gluon Sivers function in this model. The present work helps establish the stability of predictions under TMD evolution and demonstrate the dependencies of the asymmetries on the gluon Sivers function. These asymmetries probe directly the gluon Sivers function as opposed to, say, jet production, which receives contributions from both the quark induced and gluon induced processes. Therefore, study of these quarkonium asymmetries will help in determining the gluon Sivers function, just as corresponding data on heavy flavor production did for unpolarized densities.

We will present the asymmetries, in different kinematic variables, at different values of beam energies. Our results show how their energy dependence does in fact reflect the $x_g$ dependence of the gluon Sivers function. Thus, we see that the study of quarkonium asymmetries can indeed be of help in mapping the gluon Sivers function.

In this work, the color evaporation model (CEM) is used to get the cross section for the production of $J/\psi$. The details of the color evaporation model can be found in Refs. [21,22]. In Sec. II, a brief summary of the construction of the Sivers asymmetry observables is given. Section III deals with the evolution of the TMDs. In Sec. IV, we give the form of the TMDs with the evolution kernel resummed at NLL. Section V gives the details of the fits that we have used. This is followed by a summary and analysis of the results in Sec. VI.

## II. SINGLE SPIN ASYMMETRY IN $J/\psi$ PRODUCTION: FORMALISM

In the CEM, the leading-order (LO) cross section for production of $J/\psi$ is proportional to the rate of $c\bar{c}$ production integrated over the invariant mass squared of the $c\bar{c}$ pair ranging from $4m_c^2$ to $4m_D^2$ where $m_D$ is the open charm production threshold [23],

$$\sigma^{ep\to e+J/\psi+X} = \int_{4m_c^2}^{4m_D^2} dM_{c\bar{c}}^2 \int dx_\gamma\, dx_g\, f_{\gamma/e}(x_\gamma) f_{g/p}(x_g) \frac{d\hat{\sigma}^{\gamma g\to c\bar{c}}}{dM_{c\bar{c}}^2}. \tag{1}$$

Here, $f_{g/p}(x_g)$ is the gluon PDF, and $f_{\gamma/e}(x_\gamma)$ is the well-known Weiszacker–Williams function [24,25].

The SSA in the scattering of electrons off a transversely polarized proton target arises due to transverse momenta of the partons, so we use a generalized expression that takes into account the transverse momentum behavior of the Weizsacker–Williams function and the gluon PDF [18],

$$\frac{d\sigma^{e+p^{\uparrow}\to e+J/\psi+X}}{dM^2} = \int dx_\gamma\, dx_g\, d^2\boldsymbol{k}_{\perp\gamma} d^2\boldsymbol{k}_{\perp g} f_{g/p^{\uparrow}}(x_g, \boldsymbol{k}_{\perp g}) \times f_{\gamma/e}(x_\gamma, \boldsymbol{k}_{\perp\gamma}) \frac{d\hat{\sigma}^{\gamma g\to c\bar{c}}}{dM^2}, \tag{2}$$

where $M^2 \equiv M_{c\bar{c}}^2$. The difference between $d\sigma^{\uparrow}$ and $d\sigma^{\downarrow}$ is the integral over allowed phase space of the gluon Sivers function, $\Delta^N f_{g/p^{\uparrow}}(x_g, \boldsymbol{k}_{\perp g})$, weighted with $f_{\gamma/e}(x_\gamma, \boldsymbol{k}_{\perp\gamma})$ and the partonic cross section

$$d\sigma^{\uparrow} - d\sigma^{\downarrow} = \int dx_\gamma\, dx_g\, d^2\boldsymbol{k}_{\perp\gamma} d^2\boldsymbol{k}_{\perp g} \Delta^N f_{g/p^{\uparrow}}(x_g, \boldsymbol{k}_{\perp g}) \times f_{\gamma/e}(x_\gamma, \boldsymbol{k}_{\perp\gamma}) d\hat{\sigma}^{\gamma g\to c\bar{c}}. \tag{3}$$

The numerator and denominator of the asymmetry are given by [18]

$$\frac{d^4\sigma^\uparrow}{dydM^2d^2\boldsymbol{q}_T}-\frac{d^4\sigma^\downarrow}{dydM^2d^2\boldsymbol{q}_T}$$
$$=\frac{1}{s}\int d^2\boldsymbol{k}_{\perp\gamma}d^2\boldsymbol{k}_{\perp g}\Delta^N f_{g/p^\uparrow}(x_g,\boldsymbol{k}_{\perp g})f_{\gamma/e}(x_\gamma,\boldsymbol{k}_{\perp\gamma})$$
$$\times\delta^2(\boldsymbol{k}_{\perp\gamma}+\boldsymbol{k}_{\perp g}-\boldsymbol{q}_T)\hat{\sigma}_0^{\gamma g\to c\bar{c}}(M^2) \quad (4)$$

and

$$\frac{d^4\sigma^\uparrow}{dydM^2d^2\boldsymbol{q}_T}+\frac{d^4\sigma^\downarrow}{dydM^2d^2\boldsymbol{q}_T}$$
$$=\frac{2}{s}\int d^2\boldsymbol{k}_{\perp\gamma}d^2\boldsymbol{k}_{\perp g}f_{g/p}(x_g,\boldsymbol{k}_{\perp g})f_{\gamma/e}(x_\gamma,\boldsymbol{k}_{\perp\gamma})$$
$$\times\delta^2(\boldsymbol{k}_{\perp\gamma}+\boldsymbol{k}_{\perp g}-\boldsymbol{q}_T)\hat{\sigma}_0^{\gamma g\to c\bar{c}}(M^2), \quad (5)$$

where

$$x_{g,\gamma}=\frac{M}{\sqrt{s}}e^{\pm y}, \quad (6)$$

with the partonic cross section given by [17]

$$\hat{\sigma}_0^{\gamma g\to c\bar{c}}(M^2)=\frac{1}{2}e_c^2\frac{4\pi\alpha\alpha_s}{M^2}\left[\left(1+v-\frac{1}{2}v^2\right)\times\ln\frac{1+\sqrt{1-v}}{1-\sqrt{1-v}}-(1+v)\sqrt{1-v}\right]. \quad (7)$$

Here, $v=\frac{4m_c^2}{M^2}$ and $M^2\equiv\hat{s}$. We integrate Eqs. (4) and (5) over $M^2$, to obtain the difference and sum of $\frac{d^3\sigma^\uparrow}{dyd^2\boldsymbol{q}_T}$ and $\frac{d^3\sigma^\downarrow}{dyd^2\boldsymbol{q}_T}$ for $J/\psi$ production.

The sum and difference of the differential cross sections with respect to $y$ is then

$$\frac{d\sigma^\uparrow}{dy}-\frac{d\sigma^\downarrow}{dy}=\int d\phi_{q_T}\int q_T\,dq_T\int_{4m_c^2}^{4m_D^2}dM^2\int d^2\boldsymbol{k}_{\perp g}\times\Delta^N f_{g/p^\uparrow}(x_g,\boldsymbol{k}_{\perp g})f_{\gamma/e}(x_\gamma,\boldsymbol{q}_T-\boldsymbol{k}_{\perp g})\times\hat{\sigma}_0(M^2)\sin(\phi_{q_T}-\phi_S) \quad (8)$$

and

$$\frac{d\sigma^\uparrow}{dy}+\frac{d\sigma^\downarrow}{dy}=2\int d\phi_{q_T}\int q_T\,dq_T\int_{4m_c^2}^{4m_D^2}dM^2\times\int d^2\boldsymbol{k}_{\perp g}f_{g/p}(x_g,\boldsymbol{k}_{\perp g})\times f_{\gamma/e}(x_\gamma,\boldsymbol{q}_T-\boldsymbol{k}_{\perp g})\hat{\sigma}_0(M^2), \quad (9)$$

and the sum and difference of the differential cross sections with respect to $q_T$ is

$$\frac{d\sigma^\uparrow}{dq_T}-\frac{d\sigma^\downarrow}{dq_T}=\int d\phi_{q_T}\int q_T\,dy\int_{4m_c^2}^{4m_D^2}dM^2\times\int d^2\boldsymbol{k}_{\perp g}\Delta^N f_{g/p^\uparrow}(x_g,\boldsymbol{k}_{\perp g})\times f_{\gamma/e}(x_\gamma,\boldsymbol{q}_T-\boldsymbol{k}_{\perp g})\hat{\sigma}_0(M^2)\sin(\phi_{q_T}-\phi_S) \quad (10)$$

and

$$\frac{d\sigma^\uparrow}{dq_T}+\frac{d\sigma^\downarrow}{dq_T}=2\int d\phi_{q_T}\int q_T\,dy\int_{4m_c^2}^{4m_D^2}dM^2\times\int d^2\boldsymbol{k}_{\perp g}f_{g/p}(x_g,\boldsymbol{k}_{\perp g})\times f_{\gamma/e}(x_\gamma,\boldsymbol{q}_T-\boldsymbol{k}_{\perp g})\hat{\sigma}_0(M^2). \quad (11)$$

The weighted Sivers asymmetry is defined as [26]

$$A_N^{\sin(\phi_{q_T}-\phi_S)}=\frac{\int d\phi_{q_T}[d\sigma^\uparrow-d\sigma^\downarrow]\sin(\phi_{q_T}-\phi_S)}{\int d\phi_{q_T}[d\sigma^\uparrow+d\sigma^\downarrow]}, \quad (12)$$

where $d\sigma^\uparrow$ is the differential cross section in the $q_T$ or y variable, and $\phi_{q_T}$ and $\phi_S$ are the azimuthal angles of the $J/\psi$ and proton spin, respectively. For the asymmetry with respect to $y$, we use Eqs. (8) and (9) in Eq. (12). For calculating the asymmetry with respect to $q_T$, we use Eqs. (10) and (11).

The transverse momentum dependence of the Weiszacker–Williams function is taken to be Gaussian:

$$f_{\gamma/e}(x_\gamma,k_{\perp\gamma})=f_{\gamma/e}(x_\gamma)\frac{1}{\pi\langle k_{\perp\gamma}^2\rangle}e^{-k_{\perp\gamma}^2/\langle k_{\perp\gamma}^2\rangle}. \quad (13)$$

The Sivers function and the transverse momentum-dependent form of the PDF are given in Sec. IV.

## III. $Q^2$ EVOLUTION OF TMD

In this section, we present a brief outline of the energy evolution of transverse momentum-dependent functions as given in Ref. [10]. A general transverse momentum-dependent distribution $F(x,k_\perp;Q)$ can be expressed in a two-dimensional coordinate space (called $b$ space) by a fourier transform as

$$F(x,b;Q)=\int d^2k_\perp e^{-ik_\perp\cdot b}F(x,k_\perp;Q). \quad (14)$$

We will work with the $b$-space TMDs as the energy evolution is more naturally described in $b$-space. It is given by

$$F(x,b,Q_f)=F(x,b,Q_i)R_{\rm pert}(Q_f,Q_i,b_*)R_{NP}(Q_f,Q_i,b), \quad (15)$$

where $R_{\rm pert}$ is the perturbative part of the evolution kernel, $R_{NP}$ is the nonperturbative part of the kernel and $b_* = b/\sqrt{1+(b/b_{\rm max})^2}$.

The perturbative part is given by

$$R(Q_f,Q_i,b) = \exp\left\{-\int_{Q_i}^{Q_f}\frac{d\mu}{\mu}\left(A\ln\frac{Q_f^2}{\mu^2}+B\right)\right\} \times\left(\frac{Q_f^2}{Q_i^2}\right)^{-D(b;Q_i)}, \tag{16}$$

where $A=\Gamma_{\rm cusp}$ and $B=\gamma^V$, with $\frac{dD}{d\ln\mu}=\Gamma_{\rm cusp}$. The anomalous dimensions $\Gamma_{\rm cusp}$ and $\gamma^V$ are known up to three-loop level [27].

The nonperturbative exponential part, called the Sudakov factor, is fixed by fits to data. It contains a $Q$-dependent factor universal to all TMDs and another factor which gives the Gaussian width in $b$ space of the particular TMD:

$$R_{NP} = \exp\left\{-b^2\left(g_1^{\rm TMD}+\frac{g_2}{2}\ln\frac{Q_f}{Q_i}\right)\right\}. \tag{17}$$

The $b_* = b/\sqrt{1+(b/b_{\rm max})^2}$ prescription used in Eq. (15) is used to stitch together the perturbative part (which is valid at small $b$) and nonperturbative part (which is valid at large $b$). When $b \ll b_{\rm max}$, $b_* \approx b$, whereas at higher values of $b$, $b_* \approx b_{\rm max}$. As shown in Ref. [10], for consistency up to NLL, expanding the TMD $F(x,b;Q)$ at the initial scale in terms of its corresponding collinear function and keeping only the LO term, which is just the collinear PDF, we finally get

$$f_{q/H}(x,b;Q_f) = f_{q/H}(x,Q_i)\exp\left\{-\int_{Q_i}^{Q_f}\frac{d\mu}{\mu}\left(A\ln\frac{Q^2}{\mu^2}+B\right)\right\} \times\left(\frac{Q_f^2}{Q_i^2}\right)^{-D(b^*;Q_i)}\exp\left\{-b^2\left(g_1^{\rm pdf}+\frac{g_2}{2}\ln\frac{Q_f}{Q_i}\right)\right\}. \tag{18}$$

The Collins-Soper-Sterman (CSS) evolution of the Sivers function is discussed in Ref. [2]. It has been shown that the derivative of the Sivers function in $b$ space,

$$f'^{\perp}_{1T}(x,b;\mu) \equiv \frac{\partial f^{\perp}_{1T}(x,b;\mu)}{\partial b}, \tag{19}$$

satisfies the same evolution equation as the unpolarized TMD PDF. Therefore, the evolution equation is given by

$$f'^{\perp g}_{1T}(x,b;Q_f) = f'^{\perp g}_{1T}(x,b;Q_i)\exp\left\{-\int_{Q_i}^{Q_f}\frac{d\mu}{\mu}\left(A\ln\frac{Q^2}{\mu^2}+B\right)\right\} \times\left(\frac{Q_f^2}{Q_i^2}\right)^{-D(b^*;Q_i)}\exp\left\{-b^2\left(g_1^{\rm sivers}+\frac{g_2}{2}\ln\frac{Q_f}{Q_i}\right)\right\}. \tag{20}$$

Now the azimuth-dependent part of the Sivers function (in $b$-space) is [2]

$$f^{\perp q(\alpha)}_{1T}(x,b) = \frac{1}{M_p}\int d^2k_\perp e^{-i\mathbf{k}_\perp\cdot\mathbf{b}}k_T^\alpha f^{\perp q}_{1T}(x,k_\perp^2). \tag{21}$$

Expanding this in $b$, we get

$$\begin{aligned} f^{\perp q(\alpha)}_{1T}(x,b) &= \frac{1}{M_p}\int d^2k_\perp[1-ik_\perp^\beta b^\beta+\cdots]k_\perp^\alpha f^{\perp q}_{1T}(x,k_\perp^2) \\ &= -\frac{ib^\alpha}{2M_p}\int d^2k_\perp|k_\perp|^2 f^{\perp q}_{1T}(x,k_\perp^2)+\cdots \\ &= \frac{ib^\alpha}{2}T_{q,F}(x,x)+\cdots \end{aligned} \tag{22}$$

Here, $T_{q,F}$ is the twist-3 Qiu–Sterman quark-gluon correlation function. It is the first $k_T$ moment of the quark Sivers function [28,29]. This equation was obtained in Ref. [30].

Now using the relation between the azimuthal part of the Sivers function and the derivative of the Sivers function, we have [2]

$$\begin{aligned} f'^{\perp}_{1T}(x,b) &= -i\frac{M_p b}{b^\alpha}f^{\perp q(\alpha)}_{1T}(x,b) \\ &\simeq \frac{M_p b}{2}T_{q,F}(x,x). \end{aligned} \tag{23}$$

Therefore, for the Sivers function, we finally get [10]

$$\begin{aligned} f'^{\perp g}_{1T}(x,b;Q_f) = \frac{M_p b}{2}T_{g,F}(x,x,Q_i) &\times\exp\left\{-\int_{Q_i}^{Q_f}\frac{d\mu}{\mu}\left(A\ln\frac{Q^2}{\mu^2}+B\right)\right\} \\ &\times\left(\frac{Q_f^2}{Q_i^2}\right)^{-D(b^*;Q_i)} \\ &\times\exp\left\{-b^2\left(g_1^{\rm Sivers}+\frac{g_2}{2}\ln\frac{Q_f}{Q_i}\right)\right\}. \end{aligned} \tag{24}$$

## IV. CSS EVOLUTION AT NLL

$A$ and $B$ in Eqs. (18) and (24) are $\Gamma_{\rm cusp}$ and $\gamma^V$, respectively, and can be expanded perturbatively. As mentioned earlier, the expansion coefficients are known up to three-loop level. The $D$ term can also be expanded perturbatively as $D=\sum_{n=1}^{\infty}D^{(n)}(\alpha_s/n)^n$. The expansion

coefficients with the appropriate gluon anomalous dimensions at NLL are [10]

$$A^{(1)} = C_A \tag{25}$$

$$A^{(2)} = \frac{1}{2}C_F\left(C_A\left(\frac{67}{18}-\frac{\pi^2}{6}\right)-\frac{5}{9}C_A N_f\right) \tag{26}$$

$$B^{(1)} = -\frac{1}{2}\left(\frac{11}{3}C_A-\frac{2}{3}N_f\right) \tag{27}$$

$$D^{(1)} = \frac{C_A}{2}\ln\frac{Q_i^2 b^{*2}}{c^2}. \tag{28}$$

Choosing the initial scale $Q_i = c/b^*$, the $D$ term vanishes at NLL. The expressions for the TMDs therefore become

$$f_{g/p}(x,b;Q) = f_{g/p}(x,c/b^*)\exp\left\{-\int_{c/b^*}^{Q}\frac{d\mu}{\mu}\left(A\ln\frac{Q^2}{\mu^2}+B\right)\right\}\exp\left\{-b^2\left(g_1^{\rm pdf}+\frac{g_2}{2}\ln\frac{Qb^*}{c}\right)\right\} \tag{29}$$

$$f_{1T}^{\prime\perp g}(x,b;Q) = \frac{M_p b}{2}T_{g,F}(x,x,c/b^*)\exp\left\{-\int_{c/b^*}^{Q}\frac{d\mu}{\mu}\left(A\ln\frac{Q^2}{\mu^2}+B\right)\right\}\exp\left\{-b^2\left(g_1^{\rm Sivers}+\frac{g_2}{2}\ln\frac{Qb^*}{c}\right)\right\}. \tag{30}$$

This is related to the Sivers function given in Eq. (3) by

$$\Delta^N f_{g/p^\uparrow}(x_g,\boldsymbol{k}_{\perp g},Q) = -2\frac{k_{\perp g}}{M_p}f_{1T}^{\perp g}(x_g,k_{\perp g};Q)\cos\phi_{k_\perp}, \tag{31}$$

where $f_{1T}^{\perp g}(x_g,k_{\perp g};Q)$ and similarly $f(x,k_{\perp g},Q)$ can be obtained from $f_{1T}^{\prime\perp g}(x_g,b;Q)$ and $f(x,b;Q)$ by doing a Fourier transform as shown in Ref. [15]:

$$f_{g/p}(x_g,k_{\perp g};Q) = \frac{1}{2\pi}\int_0^\infty db\, bJ_0(k_{\perp g}b)f_{g/p}(x_g,b;Q) \tag{32}$$

$$f_{1T}^{\perp g}(x_g,k_{\perp g};Q) = -\frac{1}{2\pi k_{\perp g}}\int_0^\infty db\, bJ_1(k_{\perp g}b)f_{1T}^{\prime\perp g}(x_g,b;Q). \tag{33}$$

The expression for the numerator of the $y$ asymmetry is given by

$$\begin{aligned}\frac{d\sigma^\uparrow}{dy}-\frac{d\sigma^\downarrow}{dy} = &\int d\phi_{q_T}\int q_T\,dq_T\int_{4m_c^2}^{4m_D^2}dM^2\int d^2\boldsymbol{k}_{\perp g}\\ &\times\frac{1}{\pi M_p}\cos\phi_{k_\perp}\int_0^\infty dbbJ_1(k_{\perp g}b)f_{1T}^{\prime\perp g}(x_g,b;Q)\\ &\times f_{\gamma/e}(x_\gamma,\boldsymbol{q}_T-\boldsymbol{k}_{\perp g})\hat{\sigma}_0(M^2)\sin(\phi_{q_T}-\phi_S),\end{aligned} \tag{34}$$

where the $b$-space Sivers function, $f_{1T}^{\prime\perp g}(x_g,b;Q)$, is given by Eq. (30).

## V. NUMERICAL ESTIMATES

We adopt the formalism of Ref. [10] and assume that the Qiu–Sterman function is proportional to the unpolarized collinear PDFs [10,31],

$$T_{q,F}(x,x,Q) = \mathcal{N}_q(x)f_{q/P}(x,Q), \tag{35}$$

where for $\mathcal{N}_q(x)$, as in our previous work, we use the Torino parametrization:

$$\mathcal{N}_f(x) = N_f x^{a_f}(1-x)^{b_f}\frac{(a_f+b_f)^{(a_f+b_f)}}{{a_f}^{a_f}{b_f}^{b_f}}. \tag{36}$$

Here $a_f, b_f, N_f$ are free parameters obtained by fitting to data. Echevarria *et al.* have obtained these parameters by a global fit of Sivers asymmetry in SIDIS using data on kaons, pions and charged hadrons from JLab, HERMES and COMPASS. These parameters are known for $u$ and $d$ quarks, but there is no information available on $N_g$, $a_g$ and $b_g$ for gluons. In our work, we have used two parametrizations first proposed by Boer and Vogelsang [20]:

$$\begin{aligned}&\text{(a) } \mathcal{N}_g(x) = (\mathcal{N}_u(x)+\mathcal{N}_d(x))/2\\ &\text{(b) } \mathcal{N}_g(x) = \mathcal{N}_d(x).\end{aligned} \tag{37}$$

In the first choice, it is assumed that the gluon Sivers function is the average of the up and down quark Sivers functions. The second choice is based on the fact that the gluon PDF is similar to the down quark PDF. Since these choices are essentially based on certain heuristic arguments, we explore the dependence of the asymmetry on these choices by comparing the estimates obtained with both.

The latest fits performed in Ref. [10] give the following values for the parameters of the quark Sivers function and the widths of the TMDs. This set was fitted at $Q_0 = \sqrt{2.4}$ GeV. We call this set TMD-e2,

$$\begin{aligned} &N_u = 0.106, \quad a_u = 1.051, \quad b_u = 4.857, \\ &N_d = -0.163, \quad a_d = 1.552, \quad b_d = 4.857, \\ &b_{\max} = 1.5\ \text{GeV}^{-1}, \quad \langle k_{s\perp}^2 \rangle = 0.282\ \text{GeV}^2, \\ &\langle k_\perp^2 \rangle = 0.38\ \text{GeV}^2, \quad g_2 = 0.16\ \text{GeV}^2. \end{aligned} \tag{38}$$

These fits are used with the evolution formulation given above, in which the perturbative part is resummed up to NLL accuracy. Next, we include another set of parameters which we use to estimate the asymmetry, using the formulation provided in Ref. [15]. These parameters, extracted at $Q_0 = 1.0$ GeV, are for the exact solution of TMD evolution equations. We call this set TMD-e1,

$$\begin{aligned} &N_u = 0.77, \quad a_u = 0.68, \quad b_u = 3.1, \\ &N_d = -1.00, \quad a_d = 1.11, \quad b_d = 3.1, \\ &b_{\max} = 0.5\ \text{GeV}^{-1}, \quad M_1^2 = 0.40\ \text{GeV}^2, \\ &\langle k_\perp^2 \rangle = 0.25\ \text{GeV}^2, \quad g_2 = 0.68\ \text{GeV}^2. \end{aligned} \tag{39}$$

The asymmetries obtained with both parametrizations above are also compared with the results of Ref. [19] which is our previous paper where we have used an analytical solution of approximated TMD evolution equations. This analytical solution was obtained under the approximation that the perturbative part of the evolution kernel is independent of $b_T$ [15]. It should be noted that the parameter set for the analytical form is different from the one in Eq. (39). We call this TMD-a set in Figs. 2–11 and give the parameters below for completeness:

$$\begin{aligned} &N_u = 0.75, \quad a_u = .82, \quad b_u = 4.0, \\ &N_d = -1.00, \quad a_d = 1.36, \quad b_d = 4.0, \\ &b_{\max} = 0.5\ \text{GeV}^{-1}, \quad M_1^2 = 0.34\ \text{GeV}^2, \\ &\langle k_\perp^2 \rangle = 0.25\ \text{GeV}^2, \quad g_2 = 0.68\ \text{GeV}^2. \end{aligned} \tag{40}$$

In all these cases, $\langle k_\perp^2 \rangle$ is given for quarks. We use the same value for gluons. It should be noted that in the case of TMD-e1 and TMD-a fits the appropriate Sivers function given in Ref. [15] was used.

For the asymmetry estimated using TMD-e2, MSTW2008LO gluon distribution was used. In the other cases, GRV98LO gluon distribution was used. These were the respective densities used by the authors of the different fits. The TMDs were evaluated at $Q^2 = \hat{s}$, which varies from $4m_c^2$ to $4m_D^2$. Here $m_c$ is the charm quark mass, taken to be 1.275 GeV, and $m_D = 1.863$ is the "open-charm" threshold, i.e., the $D$-meson mass.

The center-of-mass energies at which the asymmetry has been estimated are as follows: $\sqrt{s} = 4.7$ GeV (JLAB), 7.2 GeV (HERMES), 17.33 GeV (COMPASS), 31.6 GeV (eRHIC-1) and 158.1 GeV (eRHIC-2).

We would like to point out that in our previous work we had calculated the kernel using the quark anomalous dimensions instead of gluon anomalous dimensions. However, as the kernel, which is independent of $b_T$ (in the analytical approximation) canceled between the numerator and the denominator of the asymmetry, this did not affect the result. In all the exact calculations here, however, we have used gluon anomalous dimensions while calculating the kernel, as one should. For completeness, in Fig. 1(a) we show a plot comparing the gluon Sivers function obtained using the quark anomalous dimensions and gluon anomalous dimensions. We note here that even in the case where we do not neglect the $b_T$ dependence of the kernel the difference in the asymmetries obtained using a gluon kernel and a quark kernel are very small. This is because the kernel, which is in convolution with other factors, is present

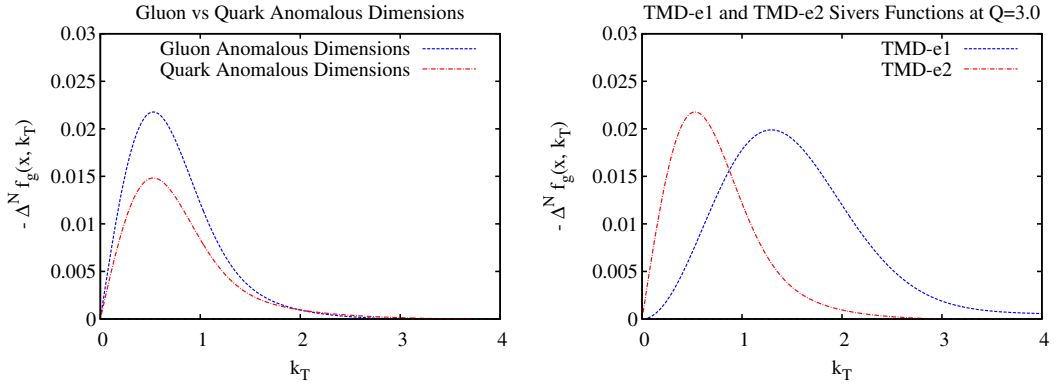


FIG. 1 (color online). Left: (a) Plot of the gluon Sivers functions in the TMD-e1 at $Q = 3.0$ obtained using gluon and quark anomalous dimensions, respectively, in the evolution kernel. Right: (b) Plot of the gluon Sivers functions at Q = 3.0 obtained two using different fits, TMD-e1 and TMD-e2. The shift in the position of the peak has implications for the $q_T$ distribution of the Sivers asymmetry.

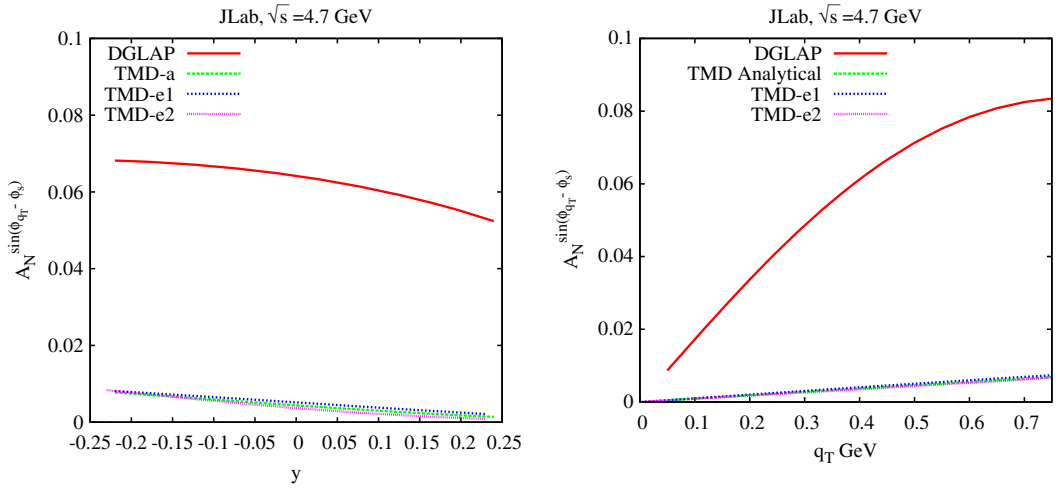


FIG. 2 (color online). The Sivers asymmetry $A_N^{\sin(\phi_{q_T}-\phi_S)}$ for $e + p^{\uparrow} \to e + J/\psi + X$ at JLab energy ($\sqrt{s} = 4.7$ GeV), as a function of $y$ (left panel) and $q_T$ (right panel) for *parametrization (a)*. The dotted green line corresponds to the TMD analytical approximated evolution approach given in Ref. [19], and the dotted blue line corresponds to exact TMD evolution approach with the TMD-e1 parameter set. The dotted pink line corresponds to the TMD evolution results using the CSS approach with the TMD-e2 parameter set, and the solid red line corresponds to the asymmetry obtained using the DGLAP evolution given in Ref. [18]. The integration ranges are $(0 \le q_T \le 1)$ GeV and $(-0.25 \le y \le 0.25)$.

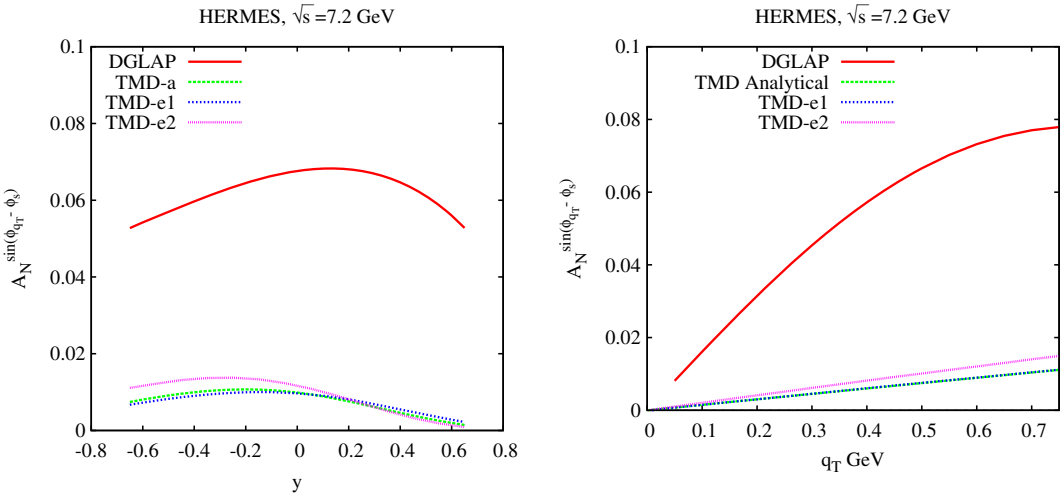


FIG. 3 (color online). HERMES energy ($\sqrt{s} = 7.2$ GeV), asymmetry as a function of $y$ (left panel) and $q_T$ (right panel) for parametrization (a). The integration ranges are $(0 \le q_T \le 1)$ GeV and $(-0.6 \le y \le 0.6)$. The convention for the color and line styles is the same as in Fig. 2.

both in the numerator and the denominator of the asymmetry and cancels out to a high degree.

In Fig. 1(b), we show the gluon Sivers function obtained using the fits TMD-e1 and TMD-e2. The Sivers function is plotted against $k_\perp$ at $Q = 3.0$ GeV. The plot clearly shows that the peak of the Sivers function in the TMD-e1 fit occurs at a higher value of $k_T$ than in the TMD-e2 fit. This has implications for the $q_T$ distribution of the Sivers asymmetry.

Next, we show the Sivers asymmetries obtained at JLab, HERMES, COMPASS , eRHIC-1 and eRHIC-2 energies for both parametrizations (a) and (b) of the Sivers function shown in Eq. (37). The asymmetry as a function of $y$ was obtained by integrating Eq. (12) over $q_T$ (from 0 to 1 GeV). We call this the "$y$ asymmetry." The asymmetry as a function of $q_T$ was obtained by integrating Eq. (12) over the kinematically allowed ranges of $y$. These were $-0.25 \le y \le 0.25$ for JLab, $-0.6 \le y \le 0.6$ for HERMES, $-1.5 \le y \le 1.5$ for COMPASS, $-2.1 \le y \le 2.1$ for eRHIC-1 and $-3.7 \le y \le 3.7$ for eRHIC-2. We call this the "$q_T$ asymmetry". It should be noted that the rapidity, $y$, given here is in the c.m. frame of the colliding electron and proton.

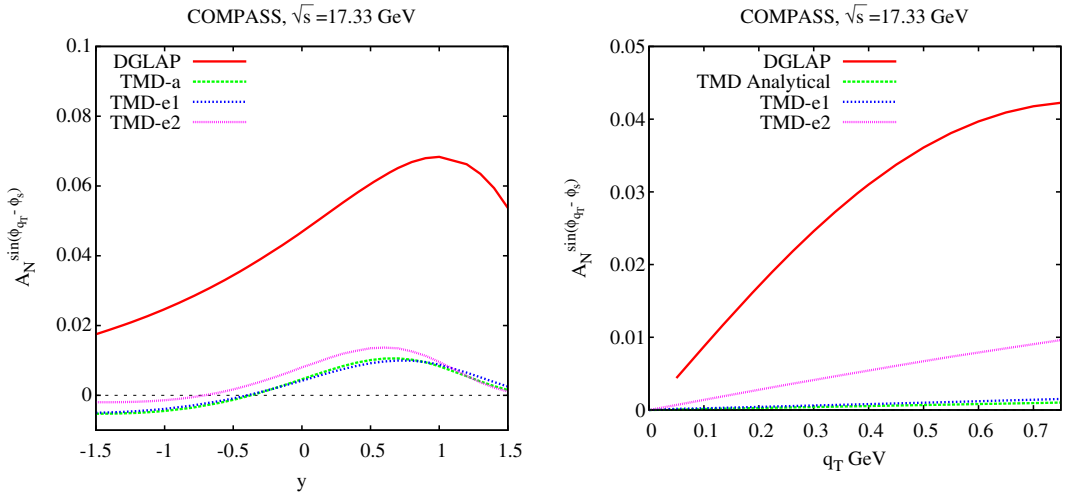


FIG. 4 (color online). COMPASS energy ($\sqrt{s} = 17.33$ GeV), asymmetry as a function of $y$ (left panel) and $q_T$ (right panel) for parametrization (a). The integration ranges are $(0 \leq q_T \leq 1)$ GeV and $(-1.5 \leq y \leq 1.5)$. The convention for the color and line styles is the same as in Fig. 2.

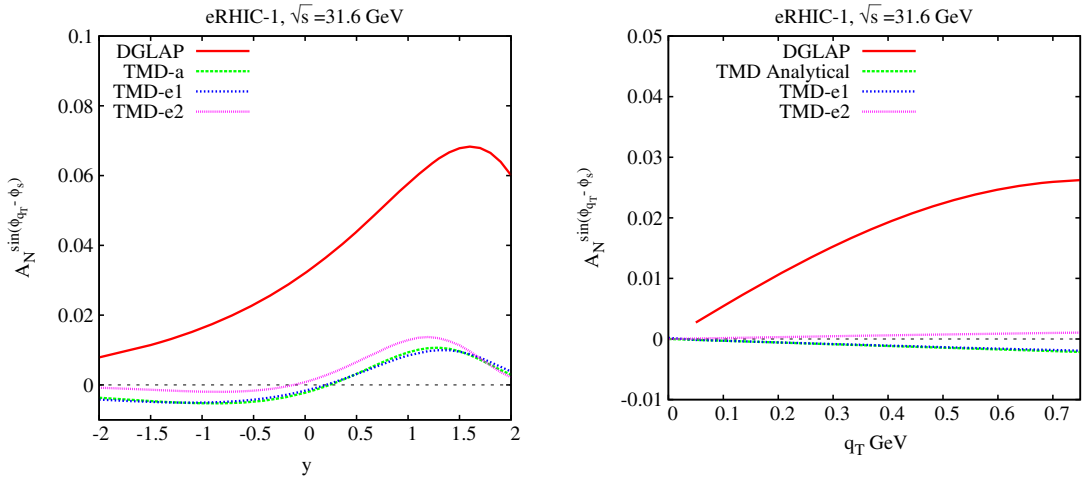


FIG. 5 (color online). eRHIC-1 energy ($\sqrt{s} = 31.6$ GeV), asymmetry as a function of $y$ (left panel) and $q_T$ (right panel) for parametrization (a). The integration ranges are $(0 \leq q_T \leq 1)$ GeV and $(-2.1 \leq y \leq 2.1)$. The convention for the color and line styles is the same as in Fig. 2.

Figures 2–6 show the asymmetries as a function of $y$ and $q_T$ with increasing c.m. energies from JLab (4.7 GeV) to e-RHIC (158.1 GeV). We do this for all three TMD evolved fits as well as the DGLAP fit with parametrization (a) of the gluon Sivers function as given in Eq. (37). Figures 7–11 show the same but for parametrization (b) of the gluon Sivers function.

Now we discuss the results in detail. We are broadly concerned with two things: The behavior of the predictions under different treatments of transverse momentum-dependent evolution and the dependence of the predictions on the center-of-mass energy $\sqrt{s}$.

First we look at the behavior under different treatments of evolution. Figures 2–6 show the $y$ and $q_T$ asymmetry estimates for JLAB, HERMES, COMPASS and eRHIC-2 energies obtained using parametrization (a) of the gluon Sivers function. Figures 7–11 show estimates obtained with parametrization (b). We can see that the asymmetries given by the TMD-a and TMD-e1 fits are similar. This was to be expected as both use the same kernel (except for the approximation on the $b_T$ dependence) and were fitted to the same data. This shows that the approximation made in obtaining the analytical solution in Ref. [15] is a good one. The $y$ asymmetries given by the TMD-e2 fits are also similar in size to the asymmetries given by TMD-a and TMD-e1 for parametrization (b) of the gluon Sivers function. However, they are slightly larger in case of parametrization (a). We would like to remind the reader

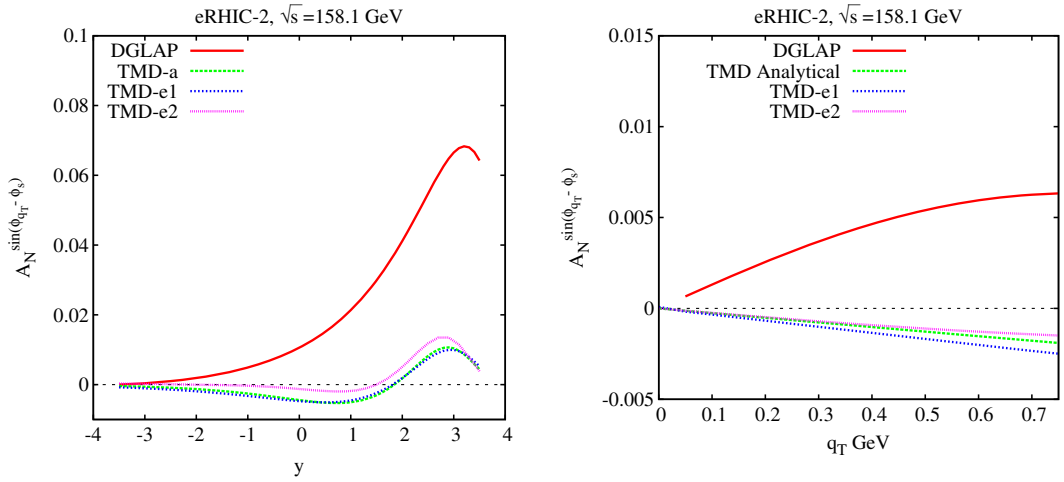


FIG. 6 (color online). eRHIC-2 energy ($\sqrt{s} = 158.1$ GeV), asymmetry as a function of $y$ (left panel) and $q_T$ (right panel) for parametrization (a). The integration ranges are $(0 \le q_T \le 1)$ GeV and $(-3.7 \le y \le 3.7)$. The convention for the color and line styles is the same as in Fig. 2.

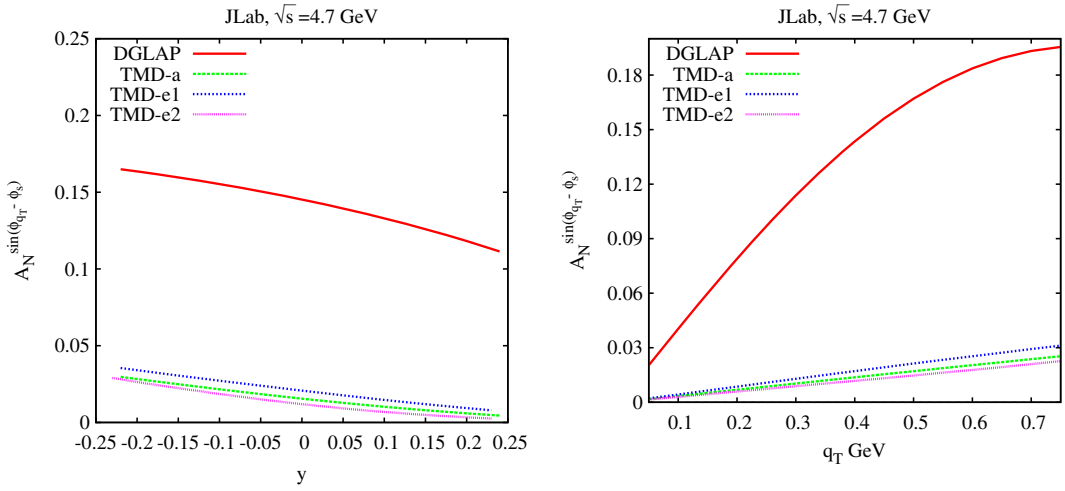


FIG. 7 (color online). JLab energy ($\sqrt{s} = 4.7$ GeV), asymmetry as a function of $y$ (left panel) and $q_T$ (right panel) for *parameterization (b)*. The integration ranges are $(0 \le q_T \le 1)$ GeV and $(-0.25 \le y \le 0.25)$. The convention for the color and line styles is the same as in Fig. 2.

here that the perturbative part of the kernel used with the TMD-e2 fit has been resummed at NLL [10]. The asymmetries obtained using all three TMD evolved fits are much smaller than those obtained using DGLAP evolution, but among themselves, they are similar in size. That is, the predictions are stable over different treatments of TMD evolution. This is the main result of our analysis.

As was the case with the $y$ asymmetries, the three TMD evolved predictions of the $q_T$ asymmetry are much smaller than the DGLAP prediction but similar among themselves. In general, the $q_T$ asymmetries for different choices of evolution vary more among each other when compared to the $y$ asymmetries, but again the asymmetries obtained using TMD-a and TMD-e1 are similar. The magnitude of the $q_T$ asymmetries increases monotonically with $q_T$ in the range considered ($0 \le q_T \le 0.75$ GeV). For parametrization (a) of the gluon Sivers function, they even become negative for eRHIC-2 energies, as can be seen in Fig. 6. This change of sign occurs only for parametrization (a) for which the $x$-dependent normalization $\mathcal{N}_g$ is an average of $\mathcal{N}_u$ and $\mathcal{N}_d$. The change of sign takes place for values of $y$ which correspond to $x_g$ values [in Eq. (6)] where the gluon Sivers function changes sign. In parametrization (a), we have taken gluon Sivers function to be proportional to the average of the up quark and down quark $\mathcal{N}_q$. Hence, the sign of Sivers function, and therefore Sivers asymmetry, depends on the relative magnitude of $\mathcal{N}_u$ and $\mathcal{N}_d$ as these two have opposite sign. The up quark contribution

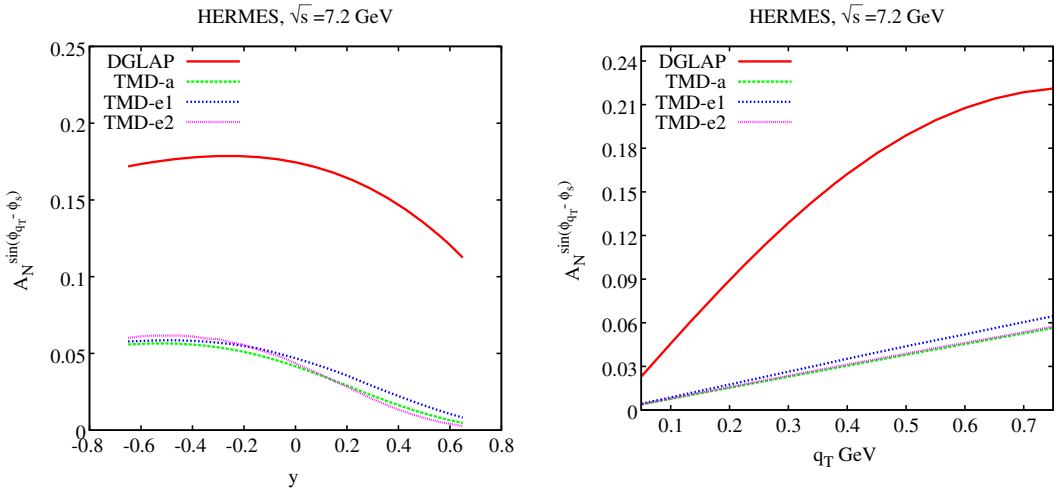


FIG. 8 (color online). HERMES energy ($\sqrt{s} = 7.2$ GeV), asymmetry as a function of $y$ (left panel) and $q_T$ (right panel) for parametrization (b). The integration ranges are $(0 \le q_T \le 1)$ GeV and $(-0.6 \le y \le 0.6)$. The convention for the color and line styles is the same as in Fig. 2.

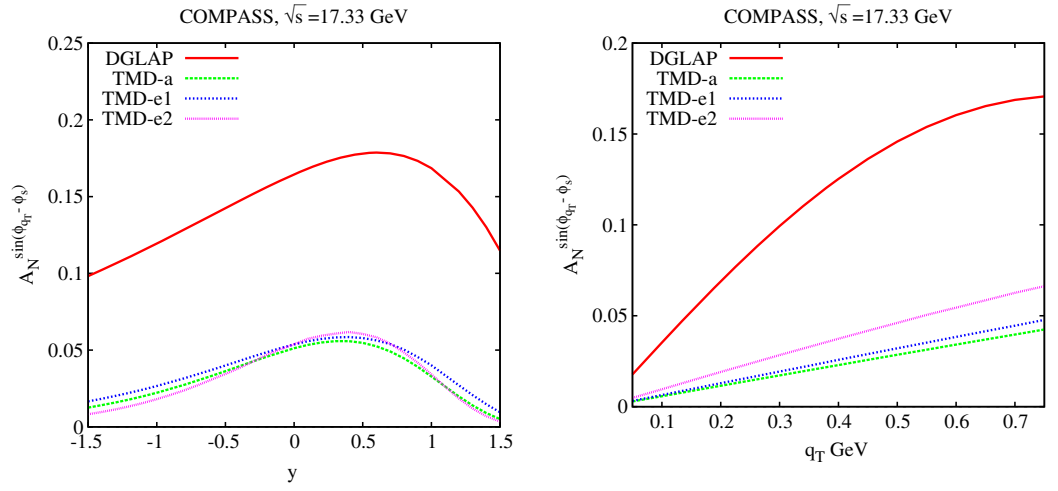


FIG. 9 (color online). COMPASS energy ($\sqrt{s} = 17.33$ GeV), asymmetry as a function of $y$ (left panel) and $q_T$ (right panel) for parametrization (b). The integration ranges are $(0 \le q_T \le 1)$ GeV and $(-1.5 \le y \le 1.5)$. The convention for the color and line styles is the same as in Fig. 2.

dominates for most of the $x_g$ values, but for small values of $x_g$, the down quark Sivers function dominates, leading to the change of sign observed herein.

The minor differences that we observe in the behavior of the $q_T$ asymmetries with different TMD fits can be understood in terms of the differences in the $k_T$ behavior of the Sivers functions obtained with different fits. Figure 1(b) shows the Sivers functions obtained using the TMD-e1 and TMD-e2 fits for $Q = 3.0$ GeV and $x = 0.1$. Since the transverse momentum behavior of the partons is directly reflected in the transverse momenta of the produced $J/\psi$ pairs, the $k_T$ behavior of the Sivers function influences the $q_T$ asymmetry.

We note that there is a substantial difference in the magnitude of the asymmetries between the two parametrizations of the gluon Sivers function. The peak asymmetry in the $y$ distribution obtained using TMD-e2 fit varies between 1.3% for parametrization (a) of the Sivers function and 6.1% for parametrization (b) for all energies except JLab. This is because the kinematics at the c.m. energy of 4.7 GeV allows contributions only from a region where the Sivers function is small. One can see from Eq. (6) that only contributions in the region $x_g \ge 0.42$ are allowed, causing only the tail end of the gluon Sivers function to affect the process.

Now we look at the dependence of the asymmetry estimates on the center-of-mass energy $\sqrt{s}$. Figure 12 shows the estimates obtained using TMD-e2 set and parametrization (a) of the gluon Sivers function, for all

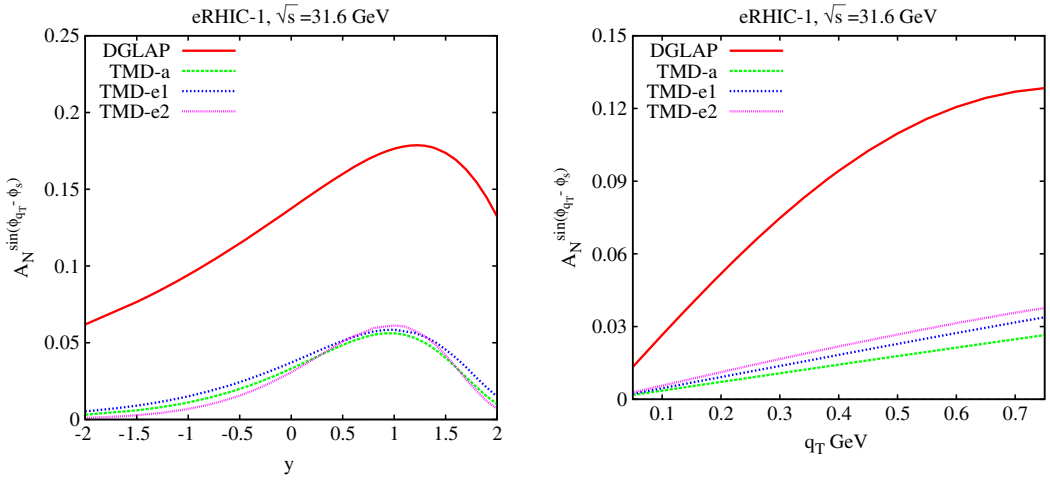


FIG. 10 (color online). eRHIC-1 energy ($\sqrt{s} = 31.6$ GeV), asymmetry as a function of $y$ (left panel) and $q_T$ (right panel) for parametrization (b). The integration ranges are $(0 \leq q_T \leq 1)$ GeV and $(-2.1 \leq y \leq 2.1)$. The convention for the color and line styles is the same as in Fig. 2.

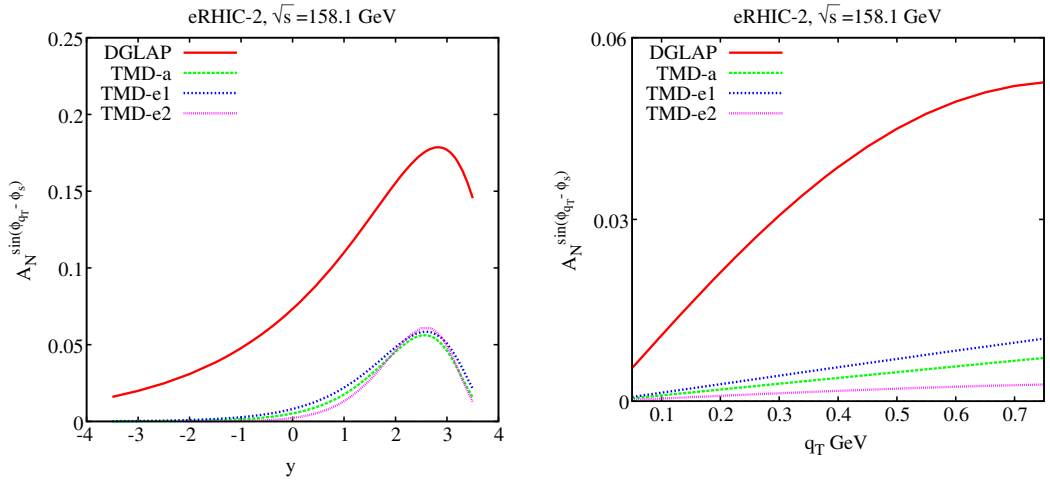


FIG. 11 (color online). eRHIC-2 energy ($\sqrt{s} = 158.1$ GeV), asymmetry as a function of $y$ (left panel) and $q_T$ (right panel) for parameterization (b). The integration ranges are $(0 \leq q_T \leq 1)$ GeV and $(-3.7 \leq y \leq 3.7)$. The convention for the color and line styles is the same as in Fig. 2.

energies. The $y$ and $q_T$ asymmetries for all considered values of $\sqrt{s}$ for the TMD-e2 fit are shown in Fig. 12. In the $y$ asymmetry, we note that the peak shifts to higher values of $y$ with increasing $\sqrt{s}$. This shift in position of the peak can be understood through the kinematic relation between $y$ and gluon momentum fraction $x_g$ and the dependence of the gluon Sivers function on $x_g$. It is clear from Eqs. (34) and (6) that the $y$ dependence of the asymmetry would reflect the $x_g$ dependence of gluon Sivers function. Putting numbers in Eq. (6), we can see that for all c.m. energies above JLab, the different values of rapidities at which the peak occurs (in the left panel of Fig. 12), correspond to a fixed value of $x_g \approx 0.3$. Since a range of invariant masses of the $c\bar{c}$ pair contribute to the quarkonium production, this value of $x_g$ which contributes most to the asymmetry can differ from the $x_g$ value where the gluon Sivers function itself peaks. Nonetheless, it is clear that the study of such scaling features at different c.m. energies can indeed shed light on the $x_g$ dependence of the gluon Sivers function, about which not much direct experimental information is available. It is to be noted further that in the case of JLab energy, however, the kinematics prevent the gluon Sivers function being probed near $x_g \approx 0.3$, and the peak is also not seen.

Apart from JLab, the asymmetry predictions in the $q_T$ distribution become smaller with increasing $\sqrt{s}$. As pointed out earlier, in the case of eRHIC energies and parametrization (a), the asymmetries even become negative.

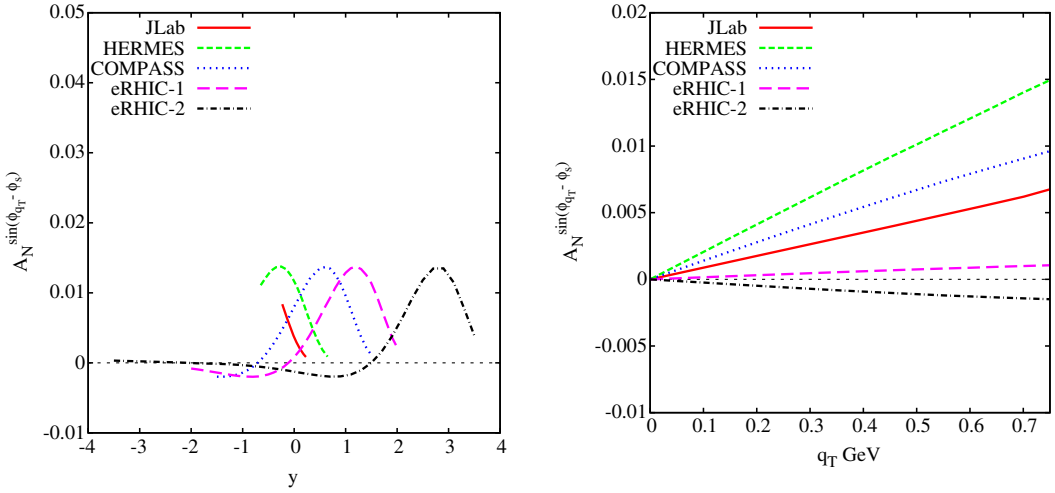


FIG. 12 (color online). Left panel: Plot of the Sivers asymmetries in the $y$ distribution obtained in all c.m. energies using the TMD-e2 fit and parametrization (a) of the gluon Sivers function. This plot shows the drift of the asymmetry peak toward higher values of rapidity $y$. Right panel: Plot of the Sivers asymmetries in the $q_T$ distribution. This shows the general decrease of asymmetry values with increasing c.m. energy. The solid red line corresponds to the asymmetry at JLAB($\sqrt{s} = 4.7$) energy, the dashed green line corresponds to HERMES($\sqrt{s} = 7.2$) energy, the dotted blue line corresponds to COMPASS($\sqrt{s} = 17.33$) energy, the dashed pink line corresponds to eRHIC-1($\sqrt{s} = 31.6$) energy, and the dashed-dotted black line corresponds to eRHIC-2($\sqrt{s} = 158.1$) energy.

The asymmetry at JLAB energy does not conform to this trend. Again, as with the $y$ distribution, this is due to the constraint on the gluon momentum fraction $x_g$.

We note that the $q_T$ asymmetries given here are for the full allowed kinematic ranges of $y$. We have not considered the acceptances of different experiments. It would be interesting to see how the predictions are affected when the details of the experiments are considered.

## VI. SUMMARY AND CONCLUSION

The single spin asymmetry in the low virtuality electroproduction of $J/\psi$ has been estimated with respect to its transverse momentum and its rapidity using a NLL-resummed TMD evolution formulation. The results for JLAB, COMPASS, HERMES, and eRHIC energies are presented at the end. It is observed that the estimates obtained are much smaller than those obtained earlier using DGLAP evolution with a nonevolving Gaussian form for the unpolarized PDF and the Sivers function. The asymmetries calculated here are also similar in size to those obtained using an earlier fit (TMD-e1) to the SIDIS data wherein the TMD evolution formalism does not include the NLL resummation. We further observe that in the case of TMD-e1 fits the difference between these asymmetries and those reported by us earlier, calculated using fits to SIDIS data based on an approximate, analytical form of the TMD evolution equation, is small. To summarize, therefore, the asymmetries obtained using the TMD evolution are consistently much smaller than those without it, and further use of the TMD evolved Sivers function stabilizes the predictions for the size of the asymmetries. Overall the asymmetries remain sizable.

## ACKNOWLEDGMENTS

We are grateful to Dr. Zhong-Bo Kang for pointing out an inconsistency in the procedure used by us. R. M. G. wishes to acknowledge support from the Department of Science and Technology, India, under Grant No. SR/S2/JCB-64/2007 under the J. C. Bose Fellowship scheme. A. M. would like to thank the Indian National Science Academy for a travel fellowship and CHEP, IISc Bangalore, for their kind hospitality. A. M. and V. S. R. would like to thank the Department of Atomic Energy-BRNS, India, for financial support under Grant No. 2010/37P/47/BRNS.

[1] S. M. Aybat and T. C. Rogers, Phys. Rev. D **83**, 114042 (2011).
[2] S. M. Aybat, J. C. Collins, J. W. Qiu, and T. C. Rogers, Phys. Rev. D **85**, 034043 (2012).
[3] P. J. Mulders and R. D. Tangerman, Nucl. Phys. **B461**, 197 (1996) [**B484**, 538 (1997)].
[4] D. W. Sivers, Phys. Rev. D **41**, 83 (1990); **43**, 261 (1991).

[5] M. Anselmino, M. Boglione, and F. Murgia, Phys. Lett. B **362**, 164 (1995); M. Anselmino and F. Murgia, Phys. Lett. B **442**, 470 (1998); M. Anselmino, M. Boglione, and F. Murgia, Phys. Rev. D **60**, 054027 (1999).
[6] J. C. Collins, *Foundations of Perturbative QCD*, Cambridge Monographs on Particle Physics, Nuclear Physics and Cosmology, No. 32 (Cambridge University Press, Cambridge, England, 2011).
[7] J. C. Collins and D. E. Soper, Nucl. Phys. **B193**, 381 (1981); **B213**, 545 (1983); X.-d. Ji, J.-p. Ma, and F. Yuan, Phys. Rev. D **71**, 034005 (2005).
[8] M. Anselmino, M. Boglione, U. D'Alesio, A. Kotzinian, F. Murgia, and A. Prokudin, Phys. Rev. D **72**, 094007 (2005); **72**, 099903 (2005).
[9] M. Anselmino, M. Boglione, U. D'Alesio, A. Kotzinian, S. Melis, F. Murgia, A. Prokudin, and C. Turk, Eur. Phys. J. A **39**, 89 (2009).
[10] M. G. Echevarria, A. Idilbi, Z.-B. Kang, and I. Vitev, Phys. Rev. D **89**, 074013 (2014).
[11] A. Airapetian *et al.* (HERMES Collaboration), Phys. Rev. Lett. **103**, 152002 (2009).
[12] M. Alekseev *et al.* (COMPASS Collaboration), Phys. Lett. B **673**, 127 (2009).
[13] C. Adolph *et al.* (COMPASS Collaboration), Phys. Lett. B **717**, 383 (2012).
[14] X. Qian *et al.* (Jefferson Lab Hall A Collaboration), Phys. Rev. Lett. **107**, 072003 (2011).
[15] M. Anselmino, M. Boglione, and S. Melis, Phys. Rev. D **86**, 014028 (2012).
[16] F. Bradamante (COMPASS Collaboration), Nuovo Cimento C **035N2**, 107 (2012).
[17] M. Gluck and E. Reya, Phys. Lett. **79B**, 453 (1978).
[18] R. M. Godbole, A. Misra, A. Mukherjee, and V. S. Rawoot, Phys. Rev. D **85**, 094013 (2012).
[19] R. M. Godbole, A. Misra, A. Mukherjee, and V. S. Rawoot, Phys. Rev. D **88**, 014029 (2013).
[20] D. Boer and W. Vogelsang, Phys. Rev. D **69**, 094025 (2004).
[21] F. Halzen, Phys. Lett. **69B**, 105 (1977); F. Halzen and S. Matsuda, Phys. Rev. D **17**, 1344 (1978).
[22] H. Fritsch, Phys. Lett. **67B**, 217 (1977).
[23] M. B. Gay Ducati and C. Brenner Mariotto, Phys. Lett. B **464**, 286 (1999).
[24] C. F. von Weizsacker, Z. Phys. **88**, 612 (1934).
[25] E. J. Williams, Phys. Rev. **45**, 729 (1934).
[26] W. Vogelsang and F. Yuan, Phys. Rev. D **72**, 054028 (2005).
[27] A. Idilbi, X.-d. Ji, and F. Yuan, Nucl. Phys. **B753**, 42 (2006).
[28] D. Boer, P. J. Mulders, and F. Pijlman, Nucl. Phys. **B667**, 201 (2003).
[29] Z.-B. Kang, J.-W. Qiu, W. Vogelsang, and F. Yuan, Phys. Rev. D **83**, 094001 (2011).
[30] Z.-B. Kang, B.-W. Xiao, and F. Yuan, Phys. Rev. Lett. **107**, 152002 (2011).
[31] C. Kouvaris, J.-W. Qiu, W. Vogelsang, and F. Yuan, Phys. Rev. D **74**, 114013 (2006).